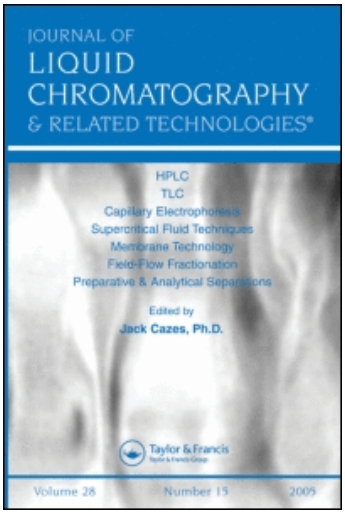

Journal of Liquid Chromatography & Related Technologies
Publication details, including instructions for authors and subscription information:
http://www.informaworld.com/smpp/title~content=t713597273

Chromatography of Suspensions - An Experimental and Theoretical Investigation of Axial Dispersion Phenomena

A. E. Hamielec[a]; S. Singh[a]
[a] Department of Chemical Engineering, McMaster University, Hamilton, Canada

To cite this Article Hamielec, A. E. and Singh, S.(1978) 'Chromatography of Suspensions - An Experimental and Theoretical Investigation of Axial Dispersion Phenomena', Journal of Liquid Chromatography & Related Technologies, 1: 2, 187 — 214
To link to this Article: DOI: 10.1080/01483917808059993
URL: http://dx.doi.org/10.1080/01483917808059993

JOURNAL OF LIQUID CHROMATOGRAPHY, 1(2), 187-214 (1978)

CHROMATOGRAPHY OF SUSPENSIONS - AN EXPERIMENTAL AND THEORETICAL INVESTIGATION OF AXIAL DISPERSION PHENOMENA

A. E. Hamielec
S. Singh
Department of Chemical Engineering
McMaster University
Hamilton, Canada L86 4L7

ABSTRACT

Herein is reported an experimental and theoretical investigation of axial dispersion phenomena in the chromatography of spherical suspensions in the submicron range. Peak separation and broadening were measured for a number of particle suspensions (polystyrene, polyvinylacetate, styrene-acrylic acid copolymer, butadiene-acrylonitrile copolymer latices and silica particles) using different column combinations containing porous inorganic packing materials (Fractosils, Bioglass, Corning Glass) and over a wide range of carrier fluid (water containing 1 g/ℓ Aerosol O.T. and 1 g/ℓ potassium nitrate) flowrates. Peak separation was virtually independent of carrier fluid flowrate while peak broadening increased significantly. Analytical solutions of the integral equation which describes axial dispersion in the chromatography of suspensions have been found for a general detector which includes light scattering, refractometer and viscosity-concentration detectors. These solutions were used to obtain dispersion corrections for various particle diameter averages (number, surface, weight and volume). Corrections to number and surface average particle diameters for axial dispersion are excessive with a light scattering detector. These large corrections are related to the fact that in the Rayleigh scattering regime, the extinction coefficient is proportional to diameter to the fourth power. The refractometer gives reasonable dispersion corrections for all particle diameter averages. The theoretical equations derived herein are equally applicable to hydrodynamic chromatography (HDC) and capillary particle chromatography (CPC).

INTRODUCTION

In the past decade, gel permeation chromatography (GPC) or liquid exclusion chromatography (LEC) has been used extensively for the separation of polymer molecules according to their size in solution. Recently, this technique has been adapted for analagous separation of spherical particles in suspension according to their size (1-8). There are two complementary approaches to the use of flow in packed beds to separate particles in suspension according to size. One technique, called liquid exclusion chromatography (LEC), utilizes porous packing and relies mainly on steric exclusion from the pores of the packing for size separation. The other called hydrodynamic chromatography (HDC) developed by Small (2,3) utilizes non-porous packing and relies mainly on the velocity profile in interstitial capillaries for size separation. Peak separation is much greater with LEC than with HDC; however, axial dispersion is also much more pronounced. Resolution depends on both peak separation and axial dispersion, and it remains to be seen which of LEC or HDC provides the greater resolution. To date, a quantitative evaluation of axial dispersion for either LEC or HDC has not been reported. In the present investigation an attempt has been made to make such a quantitative evaluation for LEC. In particular, attention

was focused on packing and pore size, carrier fluid flowrate and detector type and their influence on the magnitude of the correction for axial dispersion.

THEORETICAL DEVELOPMENT

As for macromolecules in solution, the relationship between the uncorrected detector signal and the signal corrected for axial dispersion is given by the integral equation

$$F(v) = \int_0^\infty W(y)G(v,y)dy \qquad (1)$$

where

F(v) is the uncorrected detector signal,

W(y) is the corrected detector signal,

G(v,y) is the normalized instrumental spreading function.

Equation (1) can be solved numerically to obtain W(y) given F(v) and G(v,y) (9). For the case where the instrumental spreading function may be assumed uniform, G(v,y)=G(v-y) equation (1) becomes a convolution integral

$$F(v) = \int_0^\infty W(y)G(v-y)dy \qquad (1a)$$

and taking LaPlace transformations

$$\overline{F}(s) = \overline{W}(s)\overline{G}(s) \qquad (2)$$

Provder and Rosen (10) proposed the use of a general statistical shape function to describe instrumental spreading. Employing only the term which corrects the Gaussian shape for skewing equation (2) may be written

$$\overline{F}(s) = \overline{W}(s)\exp\left(\frac{s^2\sigma^2}{2}\right)(1-\alpha s^3) \qquad (2a)$$

where σ^2 is the variance about the mean of the instrumental spreading function and α is a correction factor for skewing. When $\alpha=0$, the instrumental spreading function is Gaussian. Using appropriate values for s, $\overline{F}(s)$ and $\overline{W}(s)$ give uncorrected and corrected particle diameter averages. We will now investigate the effect of detector type on the magnitude of the correction for axial dispersion. Correction equations will be derived for a general detector which includes light scattering, refractometer and viscosity - concentration detectors.

Derivation of Axial Dispersion Corrections for a General Detector

The signal F(v) from the general detector is proportional to

$$F(v) \propto N(v)D(v)^{\gamma} \qquad (3)$$

where

N(v) is the number of particles in the detector cell at retention volume v,

D(v) is the diameter of the particles in the detector cell at retention volume v,

γ is characteristic of the detector type with $\gamma=6$ representing light scattering in the Rayleigh scattering regime and $\gamma=3$, refractometer and viscosity-concentration detectors. When $\gamma=0$, the detector signal is proportional to the number of particles and is independent of the particle size.

The uncorrected frequency distribution is given by

$$F(D)dD = \frac{-N(v)dv}{\int_0^\infty N(v)dv} = \frac{-F(v)D(v)^{-\gamma}dv}{\int_0^\infty F(v)D(v)^{-\gamma}dv} \qquad (4)$$

The definitions of some useful particle diameter averages follow

$$\bar{D}_N(uc) = \int_0^\infty F(v)D(v)^{1-\gamma}dv \Big/ \int_0^\infty F(v)D^{-\gamma}(v)dv \qquad (5a)$$

$$\bar{D}_S(uc) = \left(\int_0^\infty F(v)D(v)^{2-\gamma}dv \Big/ \int_0^\infty F(v)D(v)^{-\gamma}dv \right)^{1/2} \qquad (5b)$$

$$\bar{D}_{SS}(uc) = \int_0^\infty F(v)D(v)^{3-\gamma}dv \Big/ \int_0^\infty F(v)D(v)^{2-\gamma}dv \qquad (5c)$$

$$\bar{D}_W(uc) = \int_0^\infty F(v)D(v)^{4-\gamma}dv \Big/ \int_0^\infty F(v)D(v)^{3-\gamma}dv \qquad (5d)$$

$$\bar{D}_V(uc) = \left(\int_0^\infty F(v)D^{3-\gamma}(v)dv \Big/ \int_0^\infty F(v)D^{-\gamma}(v)dv \right)^{1/3} \qquad (5e)$$

$$\bar{D}_T(uc) = \left(\int_0^\infty F(v)D(v)^{6-\gamma}dv \Big/ \int_0^\infty F(v)D(v)^{3-\gamma}dv \right)^{1/3} \qquad (5f)$$

The above diameter averages are usually called number, surface, specific surface, weight, volume and turbidity average. Similar formulas may be written for diameter averages corrected for axial dispersion (argument c in place of uc and W(v) in place of F(v) in equations (5a)-(5f)). Assuming that the particle diameter-retention volume calibration curve can be expressed as

$$D(v) = D_1 \exp(-D_2 v), \qquad D_1, D_2 > 0 \qquad (6)$$

the various diameter averages may be expressed in terms of LaPlace transformations. For example,

$$\bar{D}_N(uc) = D_1 \bar{F}((1-\gamma)D_2) / \bar{F}(-\gamma D_2) \qquad (7a)$$

$$\bar{D}_N(c) = D_1 \bar{W}((1-\gamma)D_2) / \bar{W}(-\gamma D_2) \; . \qquad (7b)$$

Dividing equation (7b) by (7a)

$$\frac{\overline{D}_N(c)}{\overline{D}_N(uc)} = \frac{\overline{W}((1-\gamma)D_2)}{\overline{F}((1-\gamma)D_2)} \cdot \frac{\overline{F}(-\gamma D_2)}{\overline{W}(-\gamma D_2)} = \frac{\overline{G}(-\gamma D_2)}{\overline{G}((1-\gamma)D_2)} \tag{8a}$$

Introducing the expression for the instrumental spreading function, one obtains the correction factor for axial dispersion

$$\frac{\overline{D}_N(c)}{\overline{D}_N(uc)} = \exp\left(\frac{(2\gamma-1)D_2^2\sigma^2}{2}\right)\left[\frac{1+\gamma^3\alpha D_2^3}{1-(1-\gamma)^3\alpha D_2^3}\right] \tag{8b}$$

Correction factors for the other diameter averages may be derived in a similar manner and these are tabulated in Table 1. It is clear that the magnitude of the correction for axial dispersion depends on γ and therefore on detector type. To make an assessment of detector type, neglect the skewing correction by setting $\alpha=0$ and examine the dependence of the argument of the exponential on γ. Let us compare the magnitude of the corrections for a turbidity detector in the Rayleigh scattering regime ($\gamma=6$) with a refractometer ($\gamma=3$) and with a viscosity-concentration detector ($\gamma=3$). Correction factors for these detector types are given in Table 2. Correction factors for the turbidity detector are excessive for all particle diameter averages other than D_τ. This is related to the fact that the extinction coefficient is proportional to diameter to the fourth power in the Rayleigh scattering regime. A shift of the detector signal towards smaller particle (larger

TABLE 1

Axial Dispersion Correction Factors for a General Detector - Gaussian Instrumental Spreading Function Corrected for Skewing

Particle Diameter Averages	Axial Dispersion Correction Factors
$\overline{D}_N$ Number Average	$\exp\left(\frac{(2\gamma-1)D_2^2\sigma^2}{2}\right)\left(\frac{1+\gamma^3\alpha D_2^3}{1-(1-\gamma)^3\alpha D_2^3}\right)$
$\overline{D}_S$ Surface Average	$\exp\left((\gamma-1)D_2^2\sigma^2\right)\left(\frac{1+\gamma^3\alpha D_2^3}{1-(2-\gamma)^3\alpha D_2^3}\right)^{1/2}$
$\overline{D}_{SS}$ Specific Surface Average	$\exp\left(\frac{(2\gamma-5)D_2^2\sigma^2}{2}\right)\left(\frac{1-(2-\gamma)^3\alpha D_2^3}{1-(3-\gamma)^3\alpha D_2^3}\right)$
$\overline{D}_W$ Weight Average	$\exp\left(\frac{(2\gamma-7)D_2^2\sigma^2}{2}\right)\left(\frac{1-(3-\gamma)^3\alpha D_2^3}{1-(4-\gamma)^3\alpha D_2^3}\right)$
$\overline{D}_V$ Volume Average	$\exp\left(\frac{(2\gamma-3)D_2^2\sigma^2}{2}\right)\left(\frac{1+\gamma^3\alpha D_2^3}{1-(3-\gamma)^3\alpha D_2^3}\right)^{1/3}$
$\overline{D}_\tau$ Turbidity Average	$\exp\left(\frac{(2\gamma-9)D_2^2\sigma^2}{2}\right)\left(\frac{1-(3-\gamma)^3\alpha D_2^3}{1-(6-\gamma)^3\alpha D_2^3}\right)^{1/3}$

TABLE 2

Axial Dispersion Correction Factors for a Turbidity Detector in the Rayleigh Scattering Regime (γ=6) and for a Refractometer and Viscosity-Concentration Detectors (γ=3)

Particle Diameter Averages	Axial Dispersion Correction Factors	
	Turbidity Detector (γ=6)	Refractometer and Viscosity Concentration Detectors (γ=3)
$\bar{D}_N$	$\exp\left(\frac{11D_2^2\sigma^2}{2}\right)$	$\exp\left(\frac{5D_2^2\sigma^2}{2}\right)$
$\bar{D}_S$	$\exp\left(5D_2^2\sigma^2\right)$	$\exp\left(2D_2^2\sigma^2\right)$
$\bar{D}_{SS}$	$\exp\left(\frac{7D_2^2\sigma^2}{2}\right)$	$\exp\left(\frac{D_2^2\sigma^2}{2}\right)$
$\bar{D}_W$	$\exp\left(\frac{5D_2^2\sigma^2}{2}\right)$	$\exp\left(\frac{-D_2^2\sigma^2}{2}\right)$
$\bar{D}_V$	$\exp\left(\frac{9D_2^2\sigma^2}{2}\right)$	$\exp\left(\frac{3D_2^2\sigma^2}{2}\right)$
$\bar{D}_\tau$	$\exp\left(\frac{3D_2^2\sigma^2}{2}\right)$	$\exp\left(\frac{-3D_2^2\sigma^2}{2}\right)$

retention volumes) diameters causes an apparent large increase in the number of particles and large errors in particle diameter averages which depend on smaller particles. Particle diameter averages measured by the light scattering detector are always

too small. Correction factors for the refractometer and viscosity-concentration detectors are of reasonable magnitude. These correction factors will be employed with experimental data later.

Correction equations for axial dispersion for a light scattering detector in the Mie scattering regime will now be considered. The detector signal is now proportional to

$$F(v) \propto N(v)K(v)D^2(v) \tag{9}$$

where K(v) is the extinction coefficient at retention volume v. The uncorrected frequency distribution is now given by

$$F(D)dD = -\frac{F(v)K^{-1}(v)D^{-2}(v)dv}{\int_0^\infty F(v)K^{-1}(v)D^{-2}(v)dv} \tag{10}$$

and as an example, the number average particle diameter is given by

$$\bar{D}_N(c) = \int_0^\infty W(v)K^{-1}(v)D^{-1}(v)dv \Big/ \int_0^\infty W(v)K^{-1}(v)D^{-2}(v)dv \ . \tag{11}$$

To permit the use of equation (2) to derive axial dispersion correction factors, it is necessary to express particle diameter averages as LaPlace transformations. To do this, one can express the extinction coefficient as a power series in diameter fitting the numerically computed values using the Mie theory.

This operation may be expressed in terms of LaPlace transformations as

$$\bar{D}_N(c) = D_1 \sum_i \bar{W}(S_i) \Big/ \sum_j \bar{W}(s_j) = \frac{D_1 \sum_i \bar{F}(S_i)/\bar{G}(S_i)}{\sum_j \bar{F}(S_j)/\bar{G}(S_j)} \quad . \qquad (12)$$

We will now consider the experimental part of this investigation where the correction formulas derived here will be used to interpret the data.

EXPERIMENTAL DETAILS

Equipment for LEC

The instrumentation for LEC with particle suspensions is the same as for GPC with macromolecules in solution consisting of (i) Pump, (ii) sample injection valve, (iii) packed columns, (iv) detector, (v) volume counter, (vi) strip chart recorder. Details of the instrumentation employed in this investigation follow.

Sample injection valve. A conventional six port, two-way injection valve manufactured by Disc Instruments Inc. was used. This valve was designed to withstand hydrostatic pressures of up to 5000 psi. The volume of the sample loop was 2 mℓ.

Pump. A positive displacement pump (Milton Roy Mini Pump Model 396-89) with an adjustable delivery volume was used to deliver up to 7.6 mℓ/min of carrier fluid. This pump was designed to handle backpressures of up to 5000 psi. Pressure fluctuations were damped out with an inline pulse damper.

Columns. Combinations of columns (4 ft×3/8 inch) each packed with porous silica and/or glass. Details of the packing materials employed are given in Table 3. The columns were dry packed. (Columns were packed with materials having a wide range of pore sizes (30,000Å to 100Å) and particle diameters (5μ-125μ). Packing of 5-10μ were not satisfactory,as column plugging often occurred.) The following columns were packed.

Column A - Fractosil 25000 (120-230 mesh)

Column B - Fractosil 10000 (120-230 mesh)

Column C - Fractosil 5000 (120-230 mesh)

Column D - Bioglass (2500+1500+1000)(100-200 mesh)

Column E - CPG 1250 (120-200 mesh)

Column F - Waters Glass (200-800+<100)(120-200 mesh)

Column G - Bioglass (2500+1500)(100-200 mesh)

Column H - CPG 2500 (200-400 mesh)

Column I - CPG 1500 (200-400 mesh).

Detector. Most of the measurements were done using a Pharmacia UV-spectrophotometer with a cell of 10 mm pathlength

TABLE 3

Column Packings Used to Evaluate Liquid Exclusion Chromatography (LEC) with Particle Suspensions

Packing Type	Mean Pore Diameter (Å)	Particle Size (Mesh)
Fractosil 25000	30,000	120-230
(E. Merck, Darmstadt)		
Fractosil 10000	14,000	120-230
Fractosil 5000	4,900	120-230
CPG-1250	1,100	120-200
(Corning Glass Co.,		
Corning, N.Y.)		
CPG-2500	2,500	200-400
CPG-1500	1,500	200-400
Bioglass 2500	2,500	100-200
(Bio-Rad Labs.,		
Richmond, Calif.)		
Bioglass 1500	1,500	100-200
Bioglass 1000	1,000	100-200
Glass	400-800	120-200
(Waters Associates,	200-400	120-200
Milford, Mass.)	<100	120-200

and 254 nm wavelength. Later measurements were done using Waters Associates Model 440 UV-Absorbance Detector and monitoring, simultaneously, turbidities at two wavelengths.

Volume counter. A Waters liquid volume indicator with a 5 mℓ siphon was used to monitor eluent volume. To obtain an accurate measure of eluent volume, the siphon dump volume had to be corrected for carrier fluid flowrate.

Carrier fluid. The carrier fluid was distilled water containing 1 g/ℓ Aerosol OT (BDH Lab Reagent Grade) and 1 g/ℓ potassium nitrate. This carrier fluid was recommended by Coll et al. (4). No further attempt to optimize surfactant and electrolyte type or level was attempted in this investigation.

Particle standards. Monodispersed latices of different composition and silica particles with a narrow size distribution were used to establish the particle diameter-retention volume calibration curve and to show that, for the carrier fluid and packing employed, the same curve applied for all particle compositions. Specifications for the particle standards employed are given in Table 4.

Sample injection procedure. The UV-detector usually gave a steady baseline after about 20 min. from chromatograph startup. Particle standards or unknowns were diluted with the carrier fluid at room temperature, filtered through 0.8μ or 1.2μ filter paper and injected into the sample injection valve via a syringe. Solute charges were not accurately weighed,

TABLE 4

Particle Standards - Specifications

Particle Type	Diameter (microns)	Source
Polystyrene (PS)	1.011 0.760 0.481	Union Carbide Corp., South Charleston, W.Va.
	0.312 0.234	Dow Chemical Co., Midland, Michigan
	0.100	Polysciences Inc., Rydal, Pa.
	0.091	E. F. Fullam, Inc.
Styrene-methacrylic acid copolymer (SMA)	0.050	Eastman Kodak Co., Rochester, N.Y.
Silica Sol	0.250	
	0.1-0.14	
	0.05-0.08	E. I. DuPont de Nemours
Ludox TM	0.025-0.035	& Co., Wilmington,
Ludox HS	0.01-0.02	Delaware
Ludox SM	0.01-0.02	
Silica	0.022-0.025	Nalco Chemical Co., Chicago, Illinois
Silica	0.023	Sohio, Cleveland, Ohio
Butadiene-Acrylonitrile Copolymer (BD/AN)	0.14	Sohio, Cleveland, Ohio

but rather a drop or two of concentrated suspension was mixed with about 5 mℓ of carrier fluid. Typical solute charges were less than 5 mg.

RESULTS AND DISCUSSION

Peak Separation

A) Effect of particle suspension composition. A single particle diameter-retention volume calibration curve was obtained for all column combinations and particle standards employed with the carrier fluid used (water containing 1 g/ℓ Aerosol OT as anionic surfactant and 1 g/ℓ potassium nitrate as electrolyte). A typical curve showing universal calibration is shown in Figure 1.

B) Effect of carrier fluid flowrate. Increasing the carrier fluid flowrate from 0.94 mℓ/min to 7.5 mℓ/min gave an apparent shift in the particle diameter-retention volume calibration curve to smaller retention volumes without changing the slope. Figure 2 shows a typical example. However, upon correcting for the change in siphon dump volume with flowrate, the calibration curves almost superimposed (see Figure 3).

C) Effect of packing material type and size. The particle diameter-retention volume calibration curves obtained for various column combinations were linear on a semilog plot and were fit with the equation $D(v)=D_1\exp(-D_2v)$. The numerical value of D_2 is a measure of peak separation and these values

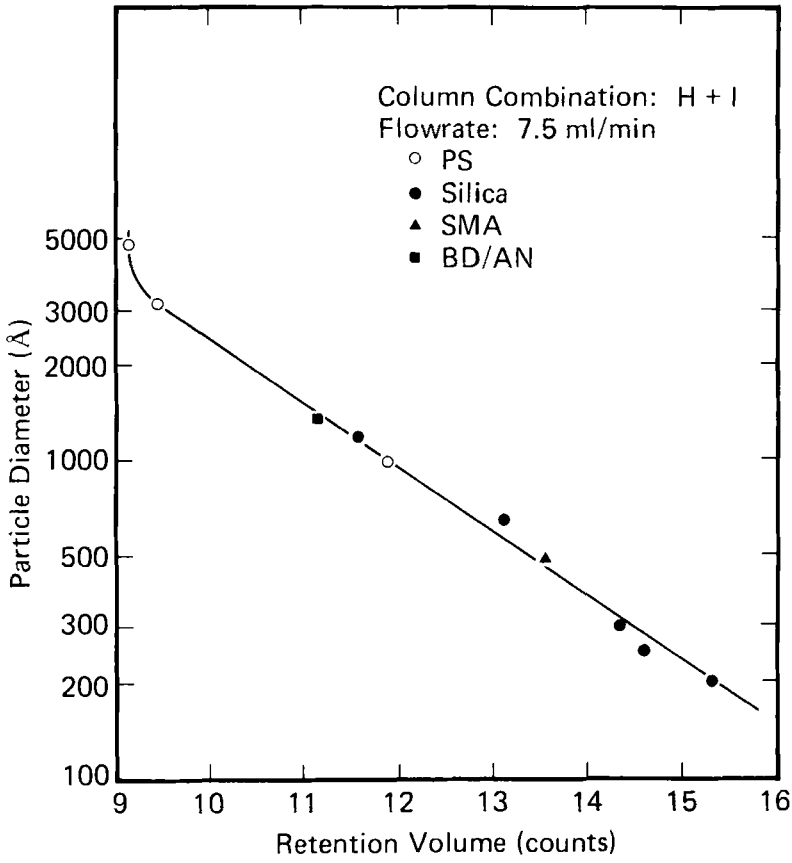

FIGURE 1

Universal particle diameter - retention volume calibration curve.

are shown tabulated in Table 5 for various column combinations (the smaller D_2, the greater is peak separation). Peak separation should be a strong function of available pore volume. However, it appears that packing particle size (compare column

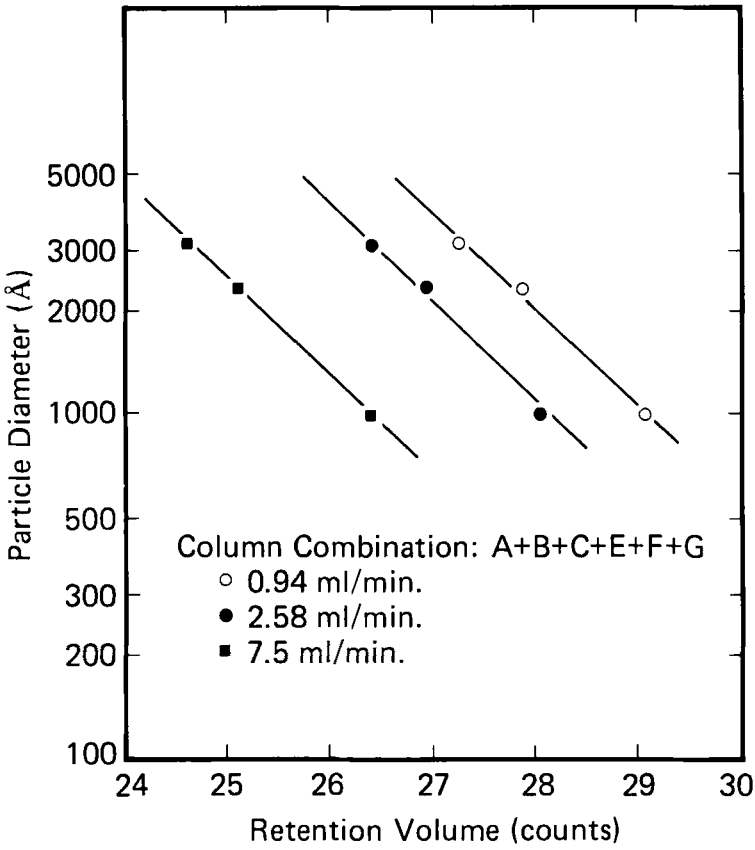

FIGURE 2

Effect of carrier fluid flowrate on particle diameter - retention volume calibration curve - retention volumes not corrected for change in siphon dump volume with flow rate.

combinations H+I and D+G) is most important. This has been shown to be the case for HDC by Small (2,3). It is a very complex situation and the available pore volume depends on the interaction of the emulsifier and electrolyte with the surface

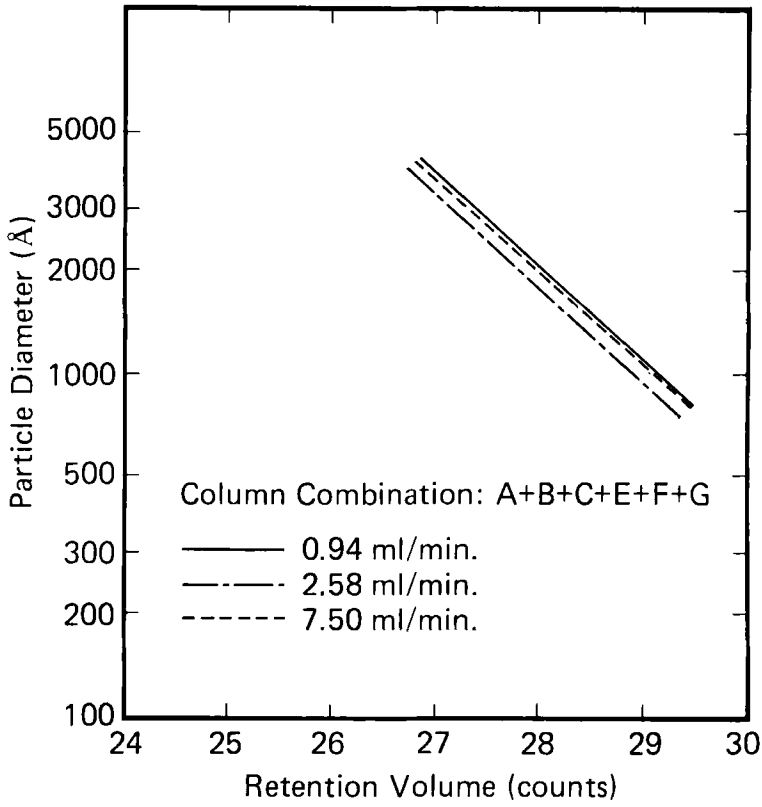

FIGURE 3

Effect of carrier fluid flowrate on particle diameter - retention volume calibration curve - retention volumes corrected for change in siphon dump volume with flowrate.

TABLE 5

Peak Separation as Measured by D_2 for Various Column Combinations

Column Combination	D_2 Counts^{-1} (1 count = 5 mℓ)
A+B+C+D+E+F	0.628
C+D+F+G	0.531
D+E+F	2.83
H+I (200-400 mesh)	0.464
D+G (100-200 mesh)	1.37

of the packing material. Coll et al. (4) have shown that significant shifts in the particle diameter-retention volume calibration curve occur when emulsifier and electrolyte concentrations are changed. With the present data it is not possible to make any unequivocal conclusions about the effect of packing type and size on peak separation.

Axial Dispersion

Chromatograms observed for the particle standards used in this investigation were close to Gaussian in shape. In the study of LEC variables on axial dispersion, all chromatograms were taken to be Gaussian and the variance about the mean measured using peak width at half height. The variance of the monodispersed standards was taken as a direct measure of axial dispersion.

A) Effect of carrier fluid flowrate. In Table 6 may be seen the effect of carrier fluid flowrate on the variance of chromatograms for PS standards 1000Å, 2340Å and 3120Å. These data are shown graphically in Figure 4. There is, initially, a significant increase in variance with carrier fluid flowrate and then a leveling off to almost a plateau. This dependence on flowrate is most likely due to the fact that at the higher flowrates the deeper pores are largely not penetrated, particularly by the larger particles. It has already been

TABLE 6

Effect of Carrier Fluid Flowrate on the Variance of Chromatograms for PS Standards 1000Å, 2340Å and 3120Å with Column Combination A+B+C+E+F+G

Carrier Fluid Flowrate (mℓ/min)	Chromatogram Variance ($m\ell^2$)		
	PS-1000Å	PS-2340Å	PS-3120Å
0.94	23.09	20.66	19.39
2.58	29.75	28.69	27.88
7.50	34.47	32.89	29.34

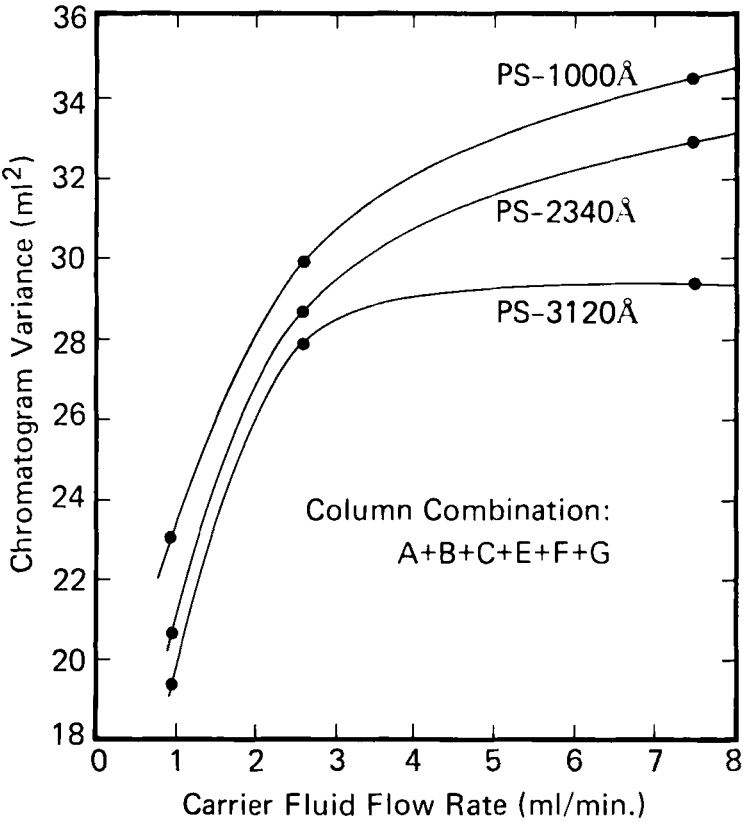

FIGURE 4

Effect of carrier fluid flowrate on chromatogram variance of monodispersed polystyrene latex standards.

observed that, with HDC, peak broadening is smaller than with LEC and that the flowrate dependence is small. It should be pointed out, however, that even for the largest particle (PS-3120Å) significant pore penetration occurs even at the largest flowrate. Appreciable peak separation and large variances may be used as evidence for this.

B) Effect of packing material type and size. Table 7 shows σ^2 and $D_2^2\sigma^2$ values for a variety of column combinations. $D_2^2\sigma^2$ can be considered a measure of resolution (see equations for axial dispersion corrections) and will be called the Resolution Index. Comparing Resolution Indices, it appears that column combinations H+I and C+D+F+G would require the smallest corrections for axial dispersion and are therefore preferred.

TABLE 7

Peak Variance and Resolution Index for Various Column Combinations at One Carrier Fluid Flowrate (~7.50 mℓ/min) of PS-1000Å

Column Combination	Chromatogram Variance ($m\ell^2$) σ^2	Resolution Index $D_2^2\sigma^2$
A+B+C+D+E+F	34.25	0.54
C+D+F+G	28.37	0.32
D+E+F	9.49	3.04
H+I	28.41	0.25
D+G	15.85	1.19

It is interesting to note that column combination D+E+F has relatively small band broadening (small variance) but, coupled with its very poor peak separation, requires an excessive correction for axial dispersion. This may indeed be the situation with HDC where peak broadening is small but peak separation poor. These results also confirm the fact that pore penetration increases both peak separation and broadening.

Reproducibility of Chromatograms

The reproducibility of peak position and variance of the chromatogram for PS-1000Å was investigated and the results are given in Table 8. These chromatograms for PS-1000Å were integrated using extinction coefficients after the Mie theory and equation (12) and its analog for the other average diameters. These results are given in Table 9.

Effect of Wavelength on Measured Particle Diameter Averages

The use of a UV-spectrophotometer at smaller wavelengths for particle detection by light scattering might conceivably be affected by chemical absorption. This possibility was investigated by employing the Waters Associates Model 440 UV-Absorbance Detector and simultaneously monitoring turbidities at wavelengths of 2540Å and 4050Å for a polystyrene latex. Polystyrene absorbs strongly at 2540Å. Particle diameter

TABLE 8

Reproducibility of Peak Position and Variance of Chromatogram of PS-1000Å with Column Combination A+B+C+E+F+G and Carrier Fluid Flowrate of 7.5 mℓ/min.

Peak Position (counts)		Particle Diameter at Peak Position (Å)	Chromatogram Variance ($m\ell^2$)
	29.32	988	31.88
	29.28	1012	35.94
	29.30	1000	33.97
	29.28	1012	35.36
	29.28	1012	34.76
Mean	29.29	1005	34.38
Std. Dev.	0.018	10.7	1.58
% Std. Dev.	0.06	1.06	4.59

TABLE 9

Reproducibility of Particle Diameter Averages of PS-1000Å Corrected for Axial Dispersion Using Analytical Solution of Convolution Integral and Mie Theory. (α=0, σ^2=1.16 counts^2 and D_2=0.464 counts^{-1}) using Column Combination H+I and Carrier Fluid Flowrate of 7.5 mℓ/min. - Turbidity Detector λ=254nm.

	$\overline{D}_N(c)$	$\overline{D}_S(c)$	$\overline{D}_{SS}(c)$	$\overline{D}_W(c)$	$\overline{D}_V(c)$	$\overline{D}_T(c)$
	791	742	667	711	716	811
	879	825	746	793	798	885
	924	877	810	848	854	926
	551	519	496	611	511	790
	712	692	708	806	697	908
Mean	771	731	685	754	715	864
Std. Dev.	148	138	118	94	130	60.2
%Std. Dev.	19.2	18.9	17.3	12.5	16.0	6.9

averages were calculated using the detector signals at these two wavelengths, and these values are compared in Table 10. The % deviations are mostly within those observed in reproducibility studies at one wavelength (see Table 9). It may therefore be concluded that chemical absorption was not significant for polystyrene latices at 2540Å wavelength.

Axial Disperions Corrections - Symmetrical and Skewing Correction Factors

Two average particle diameters, measured by electron microscopy, ($\overline{D}_N$=231Å and $\overline{D}_V$=237Å) were provided by D. L. Pytynia (Nalco Chemical Co.) for the Nalco silica standard shown in Table 4. It was therefore decided to investigate symmetrical and skewing disperions corrections using LEC with this standard. Correction equations shown in Table 1 with γ=6 were used to correct particle diameter averages obtained from the uncorrected detector signal. The uncorrected or raw chromatogram was used to estimate a variance assuming the chromatogram was Gaussian. The measured variance was approximately 1.2 counts^2 using peak width at half height. The second approach was to use the diameter averages provided by electron microscopy to estimate σ^2 and α and then correct the remaining diameter averages using these same correction parameters. These parameters were thus found to be σ^2=0.75 counts^2 and α=1.0 counts^3. The corrected diameter averages are shown in Table 11. The desirability of

TABLE 10

Effect of Wave Length on Measured Particle Diameter Averages for a Polystyrene Latex - An Investigation of Chemical Absorption using a Turbidity Detector

Average (Å)	λ=2540Å	λ=4050Å	%Deviation
$\overline{D}_N(C)$	289	274	5.1
$\overline{D}_S(C)$	266	246	7.5
$\overline{D}_{SS}(C)$	251	210	16.3
$\overline{D}_V(C)$	261	233	21.0
$\overline{D}_W(C)$	380	300	10.7
$\overline{D}_\tau(C)$	645	590	8.5

TABLE 11

Particle Diameter Averages for Nalco Silica Standard ($\overline{D}_N$=231Å and $\overline{D}_V$=237Å by Electron Microscopy) Measured by LEC Showing Corrections for Symmetrical Band Broadening and Skewing in the Raleigh Scattering Regime (D_2=0.473 counts^{-1}, σ^2 in counts^2, α in counts^3)

Diameter Averages	Un-Corrected Averages	Corrected Averages (Å) (σ^2=1.2, α=0)	Corrected Averages (Å) (σ^2=0.75, α=1.0)	Symmetrical Correction Factor	Skewing Correction Factor
$\overline{D}_N$	57	263	231	2.43	1.67
$\overline{D}_S$	59	215	231	2.24	1.75
$\overline{D}_V$	63	201	237	2.07	1.82
$\overline{D}_{SS}$	73	180	257	1.76	2.00
$\overline{D}_W$	93	177	287	1.50	2.06
$\overline{D}_\tau$	136	200	268	1.27	1.55

a skewing correction can be seen by referring to $\bar{D}_N$ and $\bar{D}_W$. By definition $\bar{D}_W$ must always be larger than $\bar{D}_N$. With the symmetrical correction alone (σ^2=1.2 and α=0) this is not the case. The skewing correction plus the symmetrical correction gives a $\bar{D}_W$ larger than $\bar{D}_N$ and also agrees with electron microscopy. The raw chromatograms usualy show some skewing with a small particle diameter tail. An alternative approach would be to fit the raw chromatogram with the instrumental spreading function to generate σ^2 and α. This approach assumes, of course, that the sample is truly monodispersed. This latter approach to estimating σ^2 and α was not used in the present investigation.

REFERENCES

1. Krebs, K. F. and Wunderlich, W., Angew. Makromol. Chem., 20, 203, 1971.
2. Small, H., J. Colloid Interface Sci., 48, 147, 1974.
3. Small, H., Saunders, F. L. and Solc., J., Adv. Colloid Interface Sci., 6, 237, 1976.
4. Coll, H., Fague, G. R. and Robillard, K. A., Exclusion Chromatography of Colloidal Dispersions, unpublished work, Eastman Kodak Co., Rochester, N.Y., 1975.
5. Gaylor, V. F. and James, H. L., Reprints - Pittsburg Conference on Analytical Chemistry, Cleveland, Ohio, 1975.

6. Singh, S. and Hamielec, A. E., "Liquid Exclusion Chromatography - A Technique for Monitoring the Growth of Polymer Particles in Emulsion Polymerization," in press, J. Applied Polymer Sci., 1977.

7. Stoisits, R. F., Poehlein, G. W. and Vanderhoff, J. W., J. Colloid Interface Sci., 57, 337, 1976.

8. McHugh, A. J., "Hydrodynamic Chromatography (HDC) for Latex Particle Size Determination," unpublished manuscript, Lehigh University, 1976.

9. Friis, N. and Hamielec, A. E., Adv. Chromatography, 13, 41, 1975.

10. Provder, T. and Rosen, E.M. ACS Preprints, Houston, 1970.